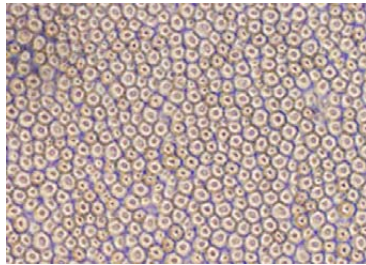
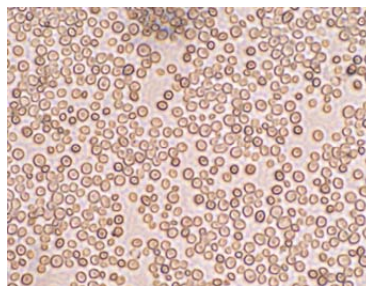


Supporting Online Material

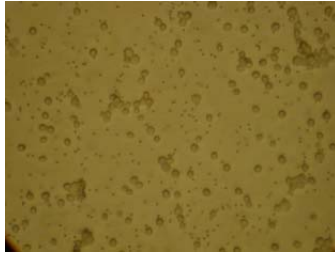
(A) Description of the supplementary movies



Movie 1: Two-directional alignment of cells using 4-point electrodes. 0.08 % w/v yeast (*S. cerevisiae*) cells were assembled into 2D arrays using an AC electric field of 75 V and 30 Hz in the four-electrode chip. The gap between opposite electrodes was ~ 18 mm. The movie is taken over 30 min at 1 frame min^{-1} .

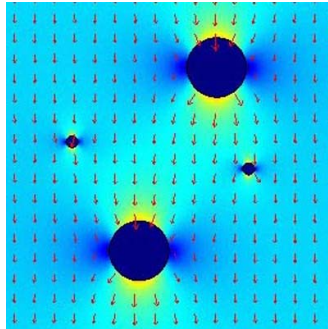


Movie 2: No structure formation in the absence of electric fields. A control test was performed in which 0.08 % w/v yeast (*S. cerevisiae*) cells were allowed to sediment under gravity in the absence of electric field. No evidence of 2D array formation was found. The movie is taken over 30 min at 1 frame min^{-1} .

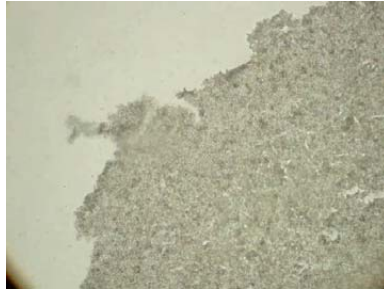


Movie 3: Experimentally observed co-assembly of yeast cells and latex particles.

0.1 % w/v yeast (*S. cerevisiae*) cells mixed with 0.1 % w/v 1 μm sulfate stabilized latex microspheres were co-assembled between two parallel coplanar electrodes. The applied AC electric field was 10 V mm^{-1} and 30 Hz. This movie has been speeded up 8 \times .



Movie 4: Numerical simulation of the co-assembly dynamics of a two cell - two particle system. 2D electrostatic simulations were performed in FEMLAB to calculate the electric field distribution and cell-particle trajectories in the system. The effective polarizability of yeast cells and 1 μm latex spheres in DI water was calculated using our computational procedure. The simulation shows how one of the latex microspheres gets entrapped between the cells due to positive dielectrophoresis.



Movie 5: 3D manipulation of permanent cell membrane. Freely suspended, one-cell layer thick, permanent yeast (*S. cerevisiae*) cell membrane was manipulated in the external field of a small magnet. This movie is in real-time.

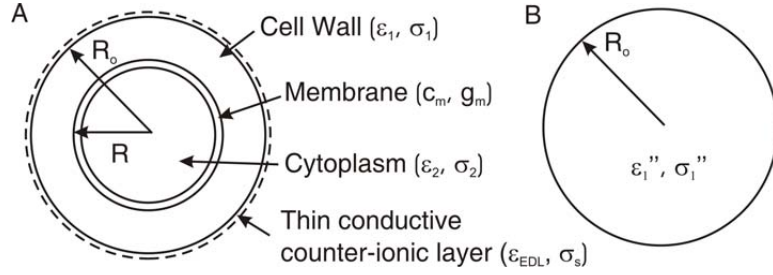


Movie 6: Folding of permanent cell membrane. Permanent and monolayer thick yeast (*S. cerevisiae*) cell membrane was folded in an external magnetic field. This movie is in real-time.

(B) Numerical simulation details

Suppl. Table 1. Numerical parameters for calculating effective polarizability of yeast (*S. cerevisiae*) cells. The values of these parameters were taken from Refs. [21, 23].

Cytoplasm dielectric constant	ϵ_2	5.31×10^{-10}	$C^2 J^{-1} m^{-1}$
Cytoplasm conductivity	σ_2	0.5	$S m^{-1}$
Membrane capacitance	c_m	0.01	$F m^{-2}$
Membrane transconductance	g_m	0	$S m^{-2}$
Cell wall dielectric constant	ϵ_1	5.75×10^{-10}	$C^2 J^{-1} m^{-1}$
Cell wall conductivity	σ_1	0.1	$S m^{-1}$
Inner radius	R	2.0×10^{-6}	m
Outer radius	R_o	2.5×10^{-6}	m
Double layer thickness	Δ	3.0×10^{-9}	m
Debye length	κ^{-1}	9.60×10^{-9}	m
Zeta potential	ζ	-30	mV
Counter-ionic layer dielectric constant	ϵ_{EDL}	1.66×10^{-12}	$C^2 J^{-1} m^{-1}$
Counter-ionic layer conductivity	σ_s	8.61×10^{-5}	$S m^{-1}$
Medium dielectric constant	ϵ_m	6.9×10^{-10}	$C^2 J^{-1} m^{-1}$
Medium conductivity	σ_m	0.017	$S m^{-1}$
Angular frequency	ω	628	$Rad s^{-1}$
Effective cell dielectric constant	ϵ_1''	1.48×10^{-8}	$C^2 J^{-1} m^{-1}$
Effective cell conductivity	σ_1''	0.039	$S m^{-1}$



Suppl. Fig. 1. (A) Multi-shell model for the polarizability of yeast cell. (B) Simplified model of yeast cell with effective polarizability equivalent to the multi-shell type structure in (A).

We developed a numerical procedure for evaluating the effective polarizability of yeast cells as a function of frequency. In this model, the multi-shelled structure of the yeast cell was substituted by a homogeneous sphere of complex permittivity

$\underline{\varepsilon}_1'' = \varepsilon_1'' - \frac{j}{\omega} \sigma_1''$ (Fig. 1B), the effective polarizability of which was equivalent to

that of the original yeast cell (Fig. 1A). The procedure includes the following steps:

1. The complex permittivities of the various shells comprising the yeast cell were expressed as follows:

$$\text{Cytoplasm:} \quad \underline{\varepsilon}_2 = \varepsilon_2 - \frac{j}{\omega} \sigma_2 \quad (1)$$

$$\text{Membrane:} \quad \underline{c}_m = c_m - \frac{j}{\omega} g_m \quad (2)$$

$$\text{Cell wall:} \quad \underline{\varepsilon}_1 = \varepsilon_1 - \frac{j}{\omega} \sigma_1 \quad (3)$$

$$\text{Counter-ionic layer:} \quad \underline{\varepsilon}_{EDL} = \varepsilon_{EDL} - \frac{j}{\omega} \sigma_s \quad (4)$$

2. The complex permittivities of the cytoplasm and the membrane were replaced with a homogeneous sphere of equivalent complex permittivity.
3. The complex permittivities of the equivalent homogeneous sphere in step 2 and the cell wall were replaced with a homogeneous sphere of equivalent permittivity.
4. The complex permittivities of the equivalent homogeneous sphere in step 3 and the thin counter-ionic layer were replaced with a homogeneous sphere of equivalent complex permittivity.

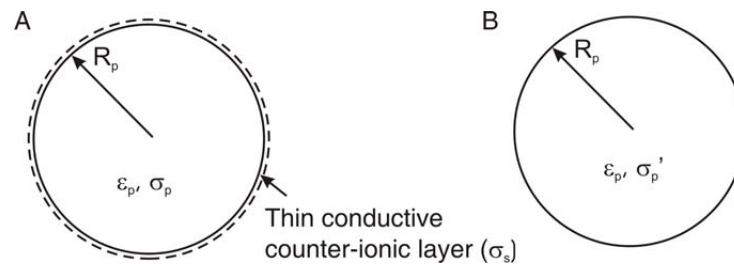
The final expression for the complex permittivity of the yeast cell in terms of the shell parameters is given by equation (5). The values of each parameter are given in Table 1.

$$\underline{\varepsilon}_1'' = \underline{\varepsilon}_1 \left[\frac{\left(\frac{R_o}{R} \right)^3 + 2 \left(\frac{\underline{\varepsilon}_2' - \underline{\varepsilon}_1}{\underline{\varepsilon}_2' + 2\underline{\varepsilon}_1} \right)}{\left(\frac{R_o}{R} \right)^3 - \left(\frac{\underline{\varepsilon}_2' - \underline{\varepsilon}_1}{\underline{\varepsilon}_2' + 2\underline{\varepsilon}_1} \right)} \right] + \underline{\varepsilon}_{EDL} \quad (5)$$

where, $\underline{\varepsilon}_2' = \frac{c_m R \underline{\varepsilon}_2}{c_m R + \underline{\varepsilon}_2}$, $\underline{\varepsilon}_{EDL} = \frac{2\Delta\varepsilon_m}{R}$ and $\sigma_s = 2\sigma_m R_o^{-1} \kappa^{-1} \exp\left(\frac{ze\xi}{2kT} - 1\right)$

Suppl. Table 2. Numerical parameters for calculating the effective polarizability of 1 μm latex particles. The values of these parameters were taken from Ref. [23] and from the information data sheet provided by the producer, Interfacial Dynamics Corp. (OR).

Particle dielectric constant	ϵ_p	2.26×10^{-11}	$\text{C}^2 \text{J}^{-1} \text{m}^{-1}$
Particle conductivity	σ_p	1.0×10^{-15}	S m^{-1}
Particle radius	R_p	5.0×10^{-7}	m
Medium dielectric constant	ϵ_m	6.95×10^{-10}	$\text{C}^2 \text{J}^{-1} \text{m}^{-1}$
Medium conductivity	σ_m	0.017	S m^{-1}
Surface charge density	γ	9.5×10^{-2}	C m^{-2}
Sodium ion mobility	μ_{Na}	5.24×10^{-8}	$\text{m}^2 \text{S C}^{-1}$
Particle surface conductivity	σ_s	0.02	S m^{-1}
Effective particle conductivity	σ_p'	0.02	S m^{-1}



Suppl. Fig. 2. Models of latex microspheres in aqueous media: **(A)** Thin conductive counter-ionic layer surrounding the latex microsphere. **(B)** Simplified structure with effective polarizability equivalent to the shell type structure in (A).

A model similar to the one described above for yeast cells was used to calculate the effective polarizability of latex particles in Fig. 2A. The equivalent conductivity of the simplified structure in Fig. 2B was given by equation (6).

$$\sigma_p' = \sigma_p + \sigma_s \quad (6)$$

where $\sigma_s = \frac{\gamma \mu_{Na}}{R}$.

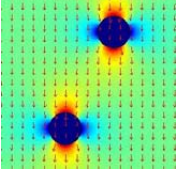
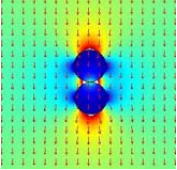
Force calculations for interactions between cells

The spherical cells and particles were modeled in the 2D electrostatic calculations using FEMLAB as thin cylinders (or disks) with a height, h , comparable to the cell diameter. We verified the accuracy of our numerical procedure by comparing its results to the analytically calculated magnitude of the dipolar interaction force between two cells. The analytical formula for dipolar interaction between spherical particles, $F_{chain} = -C\pi \varepsilon_m E^2 R^2 K^2$ (where, $3 < C < 10^3$), was modified to $F_{chain} = -C\pi \varepsilon_m E^2 R h K^2$. Here, h is the height of the cylinder and C depends on the relative positions of the two cylinders.

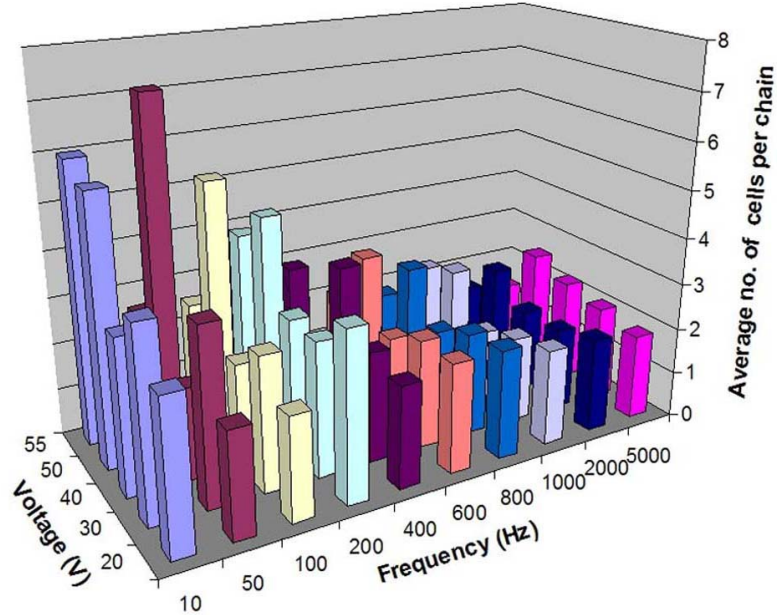
The numerical and analytical values for the dipolar attraction between two cells at different positions are given in Table 3. We assume $h = 2R$ in these calculations. The results correlated very well for the cases when the cells are separated by distances greater than $\sim 0.5R$ but a deviation of 1 - 2 orders of magnitude occurred when the cells were positioned very close to each other. This deviation is expected because the analytical

calculations do not account for the higher order mutual polarization effects that become significant at small intermolecular distances and strongly increase the attraction. The velocities of the cells after accounting for the hydrodynamic resistance were obtained to be of the order of $\sim 1 \mu\text{m s}^{-1}$, which corresponds well to the experimental data. These results suggest that the model correctly captures the dynamics and magnitudes of forces involved in the cells assembly process.

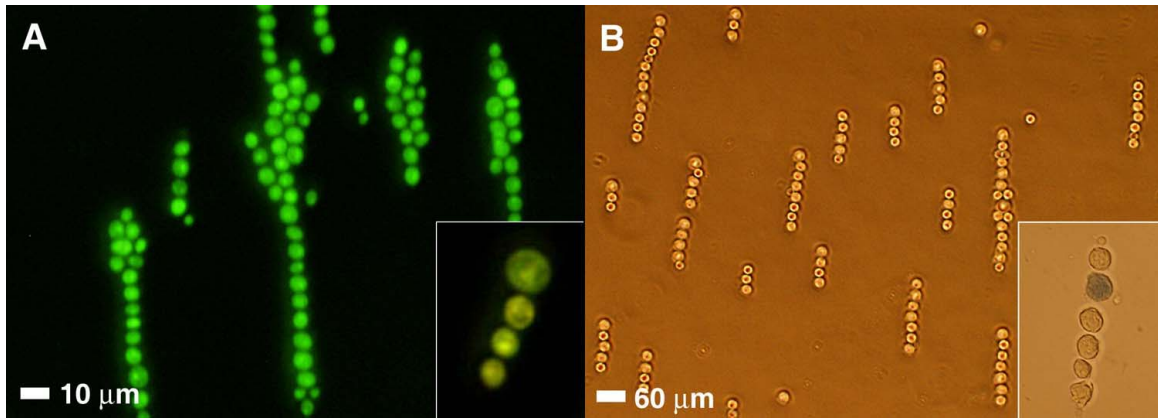
Suppl. Table 3. Force calculations for interactions between cells. Comparison between numerical and analytical values obtained for dipolar forces between yeast cells at two different positions.

<p style="text-align: center;">Dipole Interaction</p>	<p style="text-align: center;">Numerical Calculations</p> $F_{Num} = -\oint_S \left(-\frac{1}{2} E \cdot D + (n_1 \cdot E) D^T \right) dS$	<p style="text-align: center;">Analytical Calculations</p> $F_{Anal} = C \pi \varepsilon_m E^2 R h \text{Re} \left[\left(\frac{\varepsilon_c - \varepsilon_m}{\varepsilon_c + \varepsilon_m} \right)^2 \right]$
	$3.22 \times 10^{-14} \text{ N}$	$3.44 \times 10^{-14} \text{ N}$
	$1.4 \times 10^{-11} \text{ N}$	$6.25 \times 10^{-13} \text{ N}$

(C) Other supplementary data



Suppl. Fig. 3. Effect of applied AC electric field on the cell chain length. The dielectrophoretic response of 0.1 % w/v yeast (*S. cerevisiae*) cells was measured by systematically varying the voltage and frequency of the electric field between two coplanar parallel gold electrodes. The electrode gap was ~ 3 mm. 10 optical micrographs were taken at different parts of the sample exactly 2 min after turning on of the electric field. The number of cells was counted using Image Pro software (Media Cybernetics; Bethesda, MD). The results for each experiment were reported as an average of the data from ten images. The data prove that longer chains are formed at higher voltages and lower frequencies.



Suppl. Fig. 4. Cell viability tests. (A) Yeast (*S. cerevisiae*) cells were stained with FUN-1 dye and assembled into chains using 10 V mm^{-1} and 100 Hz AC electric field. The metabolic activity of cells is indicated by the orange-red fluorescent intravacuolar structures in the cytoplasm when viewed using fluorescence microscopy (inset). The micrograph shows that most cells stay alive during the assembly process. (B) NIH/3T3 mouse fibroblast cells were stained using Trypan Blue dye and aligned in 10 V mm^{-1} and 10 kHz AC electric field. Cells that do not appear blue in transmitted-mode optical microscopy are viable (inset). These results show that the viability of most fibroblast cells is unaffected by the electric field.